BIOCHEMISTRY
including biophysical chemistry & molecular biology

Article

pubs.acs.org/biochemistry

Thermal Adaptation of Dihydrofolate Reductase from the Moderate Thermophile *Geobacillus stearothermophilus*

Jiannan Guo,[†] Louis Y. P. Luk,[†] E. Joel Loveridge,[†] and Rudolf K. Allemann*[,†,‡]

[†]School of Chemistry, Cardiff University, Main Building, Park Place, Cardiff CF10 3AT, United Kingdom

[‡]Cardiff Catalysis Institute, School of Chemistry, Cardiff University, Main Building, Park Place, Cardiff CF10 3AT, United Kingdom

Supporting Information

ABSTRACT: The thermal melting temperature of dihydrofolate reductase from *Geobacillus stearothermophilus* (BsDHFR) is ∼30 °C higher than that of its homologue from the psychrophile *Moritella profunda*. Additional proline residues in the loop regions of BsDHFR have been proposed to enhance the thermostability of BsDHFR, but site-directed mutagenesis studies reveal that these proline residues contribute only minimally. Instead, the high thermal stability of BsDHFR is partly due to removal of water-accessible thermolabile residues such as glutamine and methionine, which are prone to hydrolysis or oxidation at high temperatures. The extra thermostability of BsDHFR can be obtained by ligand binding, or in the presence of salts or cosolvents such as glycerol and sucrose. The sum of all these incremental factors allows BsDHFR to function efficiently in the natural habitat of *G. stearothermophilus*, which is characterized by temperatures that can reach 75 °C.

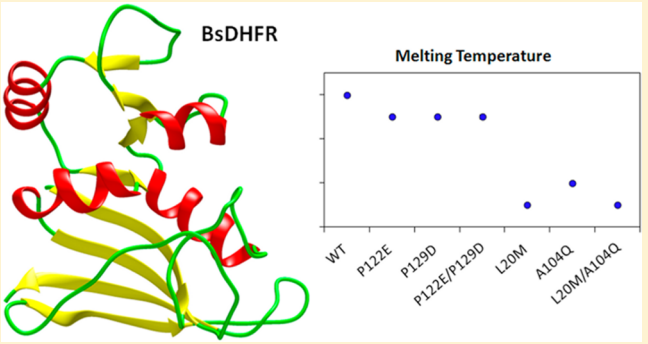

The origin of the high stability of enzymes from thermophilic organisms has been assigned to several factors that include a shortening of the loops,[1] an increased content of α-helices and β-strands,[2−4] extension of the polar surface area,[2,5,6] reduction of the total surface area through oligomerization,[7] enhanced hydrophobicity,[2] and stronger hydrogen bonding[5,6] and salt bridge interactions,[1,2,8−12] as well as an increase in the number of proline residues[2,13,14] and a reduction in the numbers of thermally labile asparagine, glutamine, methionine, or cysteine residues.[1] To design enzymes that can efficiently catalyze reactions at high temperatures, an improved understanding of the physical contributors to protein stability is essential.

Dihydrofolate reductase (DHFR) uses electrons from the cofactor NADPH to reduce 7,8-dihydrofolate (H_2F) to 5,6,7,8-tetrahydrofolate (H_4F).[15,16] Because of its ability to carry one-carbon units in different oxidation states, the product H_4F is central in many biosynthetic pathways such as the *de novo* synthesis of purine bases, deoxythymidine triphosphate, several amino acids, including methionine and glycine, and pantothenic acid in prokaryotes. Recently, a DHFR from the moderate thermophile *Geobacillus stearothermophilus* (originally named *Bacillus stearothermophilus* in 1920[17] but transferred to the genus *Geobacillus* following a reclassification in 2001[18]) has been characterized and examined with respect to its structural and kinetic adaptation to moderately high temperatures.[19−22] It can serve as a good model for studying the adaptation of thermophilic enzymes to extreme temperatures.

BsDHFR is moderately thermostable with a melting temperature at 67 °C.[21] Like other characterized DHFRs from mesophilic and psychrophilic organisms, BsDHFR is a monomer in solution and was the first monomeric DHFR from a thermophilic species to be characterized.[19] The tertiary structure of BsDHFR is closely related to that of other chromosomal DHFRs and aligns well with that of DHFR from the mesophile *Escherichia coli* (EcDHFR) (Figure 1). The M20 loop of apo-BsDHFR, which forms part of the active site, adopts a conformation similar to the "closed" M20 loop conformation in the reactant complexes of EcDHFR.[23] All elements of secondary structure can be superimposed with the closed conformation of EcDHFR except for helix E, which in BsDHFR is tilted 20° away from the adenosine binding site. The M20 loop in apo-BsDHFR does not align well with that of apo-EcDHFR because this loop is disordered in the latter case.[23,24]

The features that contribute to the stability of thermophiles have previously been discussed on the basis of a comparison of the thermophilic BsDHFR to mesophilic EcDHFR. It has been suggested that the thermal stabilization of BsDHFR is due to the extension of α-helices and β-strands (α-helix E and β-strands B, C, and E) and the insertion of prolines into loop regions (loops CD and GH).[19] The structural flexibility of BsDHFR has also been compared with that of EcDHFR.

Received: February 24, 2014
Revised: April 11, 2014
Published: April 14, 2014

   dx.doi.org/10.1021/bi500238q | *Biochemistry* 2014, 53, 2855−2863

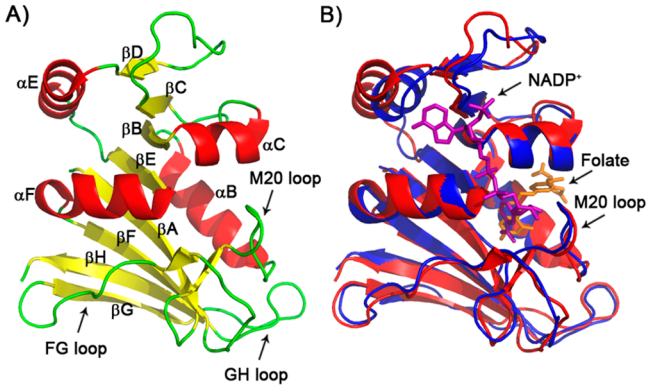

Figure 1. (A) Cartoon representation of the crystal structure of apo-BsDHFR (PDB entry 1ZDR)[19] and (B) overlay of apo-BsDHFR (red) with the closed conformation of EcDHFR (blue, PDB entry 1RX2).[23] Secondary structural elements are indicated, and ligands in EcDHFR are shown as sticks.

Interestingly, BsDHFR has a rigid core but appears to display an overall pico- to nanosecond time-scale flexibility higher than that of EcDHFR.[20,22] However, the extent to which each of these factors influences the thermostability and flexibility of BsDHFR has not yet been addressed.

The amino acid sequence of BsDHFR is 38% identical with that of EcDHFR but 44% identical with that of DHFR from the psychrophile *Moritella profunda* (MpDHFR), although the melting temperature of MpDHFR is ∼30 °C lower than that of BsDHFR.[25] Hence, the role of individual amino acids in the thermostability of BsDHFR was investigated here by site-directed mutagenesis by replacing them with the equivalent residues in MpDHFR. While apo-BsDHFR denatures at approximately 67 °C,[21] *G. stearothermophilus* can thrive at temperatures as high as 75 °C,[26] and additional environmental factors must help maintain the folded structure of BsDHFR *in vivo*.

MATERIALS AND METHODS

Chemicals. All salts and cosolvents were purchased from Sigma-Aldrich. NADPH was purchased from Melfold. NADPD was synthesized by enzymatic reduction of $NADP^+$ (Melford) using the alcohol dehydrogenase from *Thermoanaerobacter brockii* with d_8-2-propanol as the deuteride source.[27] H_2F was prepared by dithionite reduction of folic acid (Sigma-Aldrich).[28] The concentrations of NADPH(D) and H_2F were determined spectrophotometrically using extinction coefficients of 6200 cm^{-1} M^{-1} at 339 nm[29] and 28000 cm^{-1} M^{-1} at 282 nm,[30] respectively. Synthetic oligonucleotides were purchased from Eurofins MWG Operon.

Site-Directed Mutagenesis. BsDHFR variants were generated using the Phusion Site-Directed Mutagenesis Kit (New England Biolabs) following the manufacturer's instruction from a pJGetit-based vector harboring the gene encoding BsDHFR.[25] The BsDHFR gene was purchased from Epoch Biolabs. Mutagenic primers for generating BsDHFR-L20M, BsDHFR-A104Q, BsDHFR-P122E, and BsDHFR-P129D were 5′-GTAAGGATAACCGCATGCCGTGGCACCTGC-3′, 5′-CGCAGAGCTGTTTCGCCAGACCATGCCGATTGTC-3′, 5′-CTAAGATCTTTGCATCTTTCGAAGGGGATACTTTC-TATCCAC-3′, and 5′-GGGGATACTTTCTATCCAGATAT-TTCTGATGACGAATGG-3′, respectively (changes underlined). The sequences of BsDHFR variants were verified by automated DNA sequencing (Molecular Biology Unit, Cardiff University).

Protein Expression and Purification. For the production of BsDHFR and its variants, *E. coli* BL21(DE3) cells were transformed with the respective plasmid and grown to an OD_{600} of 0.6 in LB medium containing ampicillin (100 μg/mL). Expression was induced by adding isopropyl β-D-thiogalactopyranoside (IPTG) to a final concentration of 1 mM. Cells were grown overnight at 30 °C and harvested by centrifugation. Wild-type BsDHFR was heat-precipitated at 55 °C to remove *E. coli* proteins. The variants of BsDHFR were not heat treated because of their lower thermal stability. Supernatant solutions were applied to SP-Sepharose cation exchange resin pre-equilibrated in 50 mM citrate buffer (pH 5.0) and then eluted with a NaCl gradient (0 to 1 M) as described previously,[19] leading to essentially pure proteins as judged by sodium dodecyl sulfate−polyacrylamide gel electrophoresis. Protein concentrations were determined spectroscopically using an extinction coefficient of 25565 cm^{-1} M^{-1} at 280 nm.[31]

Circular Dichroism (CD) Spectroscopy. CD spectroscopy was conducted on an Applied PhotoPhysics Chirascan spectrometer. CD spectra were measured between 200 and 280 nm for enzyme (5 μM) in degassed potassium phosphate buffer (10 mM, pH 7.0). The observed ellipticities were converted to mean residue ellipticities (MRE) using the equation $[\Theta]_{MRE} = \Theta/(10ncl)$, where Θ is the ellipticity in millidegrees, n is the number of backbone amide bonds, c is the protein concentration in moles per liter, and l is the path length in centimeters. CD unfolding measurements were performed at 208 nm between 4 and 96 °C and spectra recorded in steps of 0.5 °C. The reaction buffer was incubated at each temperature for 5 min before the measurement of the spectrum. A blank run was always first performed using the buffer alone (containing the appropriate concentration of ligand where appropriate). Melting temperatures were extracted by fitting the data to an appropriate sigmoidal curve using the spectrometer software.

Kinetic Measurements. All kinetic experiments at pH 7 were performed in 100 mM potassium phosphate buffer containing 100 mM NaCl and 10 mM β-mercaptoethanol. Salt concentrations of 0.1, 0.2, 0.5, 1, 1.5, and 2 M were used for the salt effect measurements. Cosolvent concentrations of 17, 33, and 50% were used for cosolvent effect measurements. The pH was adjusted after the addition of salts and cosolvents. Details of dielectric constants and viscosities of solvent mixtures are from ref 32.

Steady-state kinetic measurements were performed on a JASCO V-660 spectrophotometer directly under saturating concentrations of NADPH (200 μM) and H_2F (100 μM). The enzyme activity was monitored spectrophotometrically at 340 nm [ε_{340} (cofactor + substrate) = 11800 M^{-1} cm^{-1}].[33] The reaction buffer was preincubated at the desired temperature, and the temperature in the cuvette was monitored immediately prior to data acquisition. The enzyme (20−50 nM) and NADPH (10−400 μM) were incubated together for 1 min, and the reaction was initiated by addition of dihydrofolate (1−100 μM). When the concentration of NADPH was varied, that of H_2F was maintained at a saturating level and vice versa. Initial linear rates of absorbance change were fit using the software provided (JASCO Corp.). The kinetic parameters k_{cat} and K_M were determined by fitting the change in the observed rate with substrate or cofactor concentration to the Michaelis−Menten equation using SigmaPlot 10.

dx.doi.org/10.1021/bi500238q | *Biochemistry* 2014, 53, 2855−2863

Pre-steady-state kinetic experiments were performed on a Hi-Tech Scientific stopped-flow spectrophotometer. Hydride transfer rate constants were measured by monitoring the fluorescence resonance energy transfer (FRET) from protein to NADPH. The sample was excited at 297 nm and the emission measured using an output filter with a cutoff at 400 nm. To avoid hysteresis, NADPH was preincubated with DHFR for 5 min at the desired temperature in a thermostated syringe compartment and the reaction initiated by rapidly mixing the sample with H_2F. Final assay conditions were 20 μM DHFR, 8 μM NADPH(D), and 100 μM H_2F. To analyze the kinetic data, a single-exponential fit was used.

RESULTS AND DISCUSSION

Design of BsDHFR Variants. In contrast to the differing thermostability, an alignment of BsDHFR, EcDHFR, and MpDHFR reveals a high degree of sequence conservation, particularly in the N-terminal region (Figure 2). The sequence

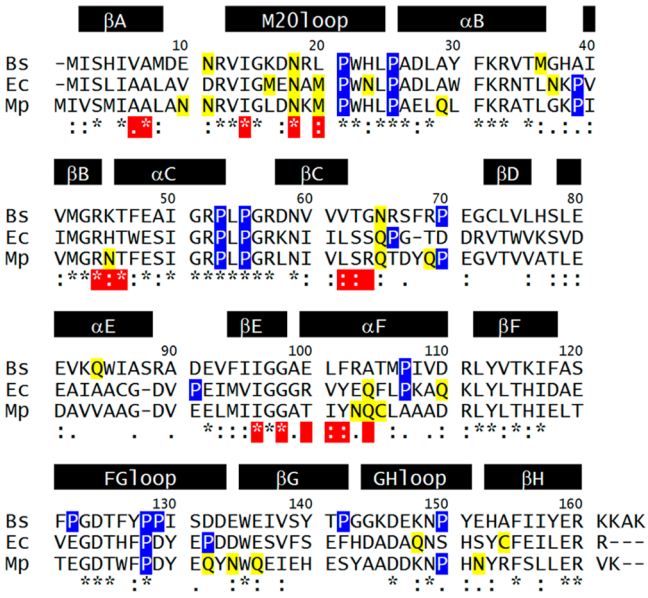

Figure 2. Sequence alignment (created using ClustalW[51]) of BsDHFR, EcDHFR, and MpDHFR. The asterisks, colons, and periods below the alignment indicate fully, strongly, and weakly conserved residues, respectively. Water-accessible thermolabile residues are highlighted in yellow. Proline residues are highlighted in blue. Red boxes below the alignment indicate the residues that contact NADPH in *E. coli* (PDB entry 1RX2).[23] The secondary structure is also indicated.

of BsDHFR is 44 and 38% identical with those of MpDHFR and EcDHFR, respectively. In particular, many residues participating in binding of the substrate (Leu28, Phe31, Lys31, and Ile96) and cofactor (Ala7, Ile14, Asn18, Arg44, Thr46, Ile96, and Gly98) are fully conserved. Interestingly, the sequence of BsDHFR is more identical to that of the psychrophilic analogue MpDHFR than to that of EcDHFR. Hydrogen−deuterium exchange experiments suggested that BsDHFR is more rigid than MpDHFR at room temperature, especially in the protein core and loop subdomain.[21,34] The higher rigidity of the loop regions of BsDHFR may be due to additional proline residues.[19] There are 11 proline residues in BsDHFR and 8 in MpDHFR, 7 of which are conserved. Two of the nonconserved proline residues in BsDHFR (Pro107 and Pro142) are in regions of secondary structure (α-helix F and β-strand G, respectively). The other two, Pro122 and Pro129, can be found in the FG loop and may contribute to the increased thermostability of BsDHFR. These residues are substituted with Glu and Asp in MpDHFR and EcDHFR, respectively. To investigate the influence of proline residues on the thermostability and catalysis of BsDHFR, variants BsDHFR-P122E and BsDHFR-P129D were prepared.

Another factor that may contribute to the thermostability of BsDHFR is the presence of fewer thermolabile residues in water-accessible regions. In a high-temperature environment, asparagine and glutamine are prone to deamidation and can induce cleavage of the peptide backbone, whereas methionine and cysteine become more sensitive to oxidation.[35] These amino acids are less common in thermophilic proteins or are buried within the protein to prevent unwanted reactions.[1] Indeed, BsDHFR and MpDHFR differ in the number of water-accessible thermolabile residues. Moreover, several residues involved in the binding of the cofactor are different from those in MpDHFR. Noticeably, Met20 and Gln104 in MpDHFR, which are conserved in many DHFRs, are substituted with Leu and Ala in BsDHFR, respectively. Therefore, variants BsDHFR-L20M and BsDHFR-A104Q were prepared to investigate the influence of thermolabile residues on the thermostability and catalysis of BsDHFR.

Conformational Analysis by CD Spectroscopy. Far-UV CD spectroscopy of BsDHFR showed characteristics of a folded structure with well-defined secondary structural elements. There is a broad negative peak at 222−208 nm for BsDHFR (Figure 3A) with a minimal mean residue ellipticity (MRE) of −6553 deg cm^2 dmol^{-1} at 209 nm. The CD spectra of all variants had similar shapes and shared a minimum at around 208 nm at 20 °C (Figure 3A). This suggests that the secondary structures of the variants are similar to that of wild-type BsDHFR.

The effects of salts and cosolvents on the secondary structure were also monitored by CD spectroscopy. Even in the presence of 2 M salts (NaCl, KCl, and KF), no major differences in the shape or intensity in the protein CD spectrum were observed, suggesting that in this concentration range Na^+, K^+, Cl^-, and F^- ions do not alter the secondary structure of the protein (Figure 3B). BsDHFR can also maintain its secondary structure in most organic cosolvents, except in tetrahydrofuran (THF) (Figure 3C). Some loss of structure was observed in the presence of 50% THF, as has been seen for EcDHFR and MpDHFR.[34,36]

Thermostability. To determine the effect of the mutations, salts, and cosolvents on the thermal stability of BsDHFR, melting temperatures were measured by monitoring the change in MRE at 208 nm with increasing temperature (Table 1). T_m was determined to be 66.2 ± 0.4 °C for wild-type, unliganded BsDHFR, which is similar to the value reported previously.[21] The binding of ligands to BsDHFR helped stabilize the protein at higher temperatures, while the melting temperatures of the BsDHFR variants are lower than that of the wild-type enzyme (Table 1). Variants with thermally labile residues incorporated (BsDHFR-L20M, BsDHFR-A104Q, and BsDHFR-L20M/A104Q) are slightly more sensitive to thermal destabilization, showing a 3−5 °C decrease in the melting temperature. Conversely, proline residues in the loop regions of BsDHFR do not contribute significantly to the thermal stability, as the melting temperatures of BsDHFR-P122E, BsDHFR-P129D, and BsDHFR-P122E/P129D decrease by only 1−2 °C.

The addition of salts had a stabilizing influence on BsDHFR (Table 2). The melting temperature of BsDHFR increased

dx.doi.org/10.1021/bi500238q | *Biochemistry* 2014, 53, 2855−2863

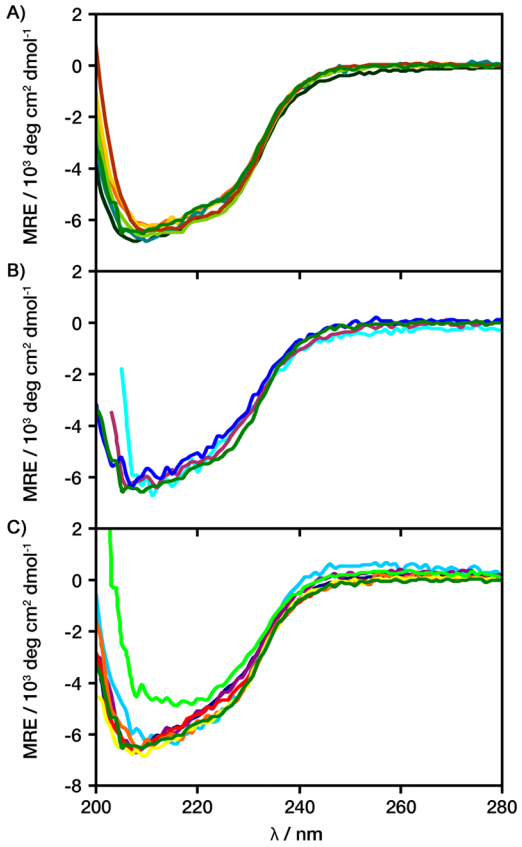

Figure 3. CD spectra of (A) BsDHFR and its variants (green for wild-type BsDHFR, orange for BsDHFR-L20M, gold for BsDHFR-A104Q, brown for BsDHFR-L20M/A104Q, dark green for BsDHFR-P122E, teal for P129D, and yellow-green for BsDHFR-P122E/P129D) at 20 °C, (B) BsDHFR at 20 °C in the presence of 2 M salts (green denotes no added salt, cyan NaCl, purple KCl, and blue KF), and (C) BsDHFR at 20 °C in the presence of 50% organic cosolvents [light blue for methanol, dark blue for ethanol, purple for 2-propanol, red for ethylene glycol, orange for glycerol, yellow for sucrose (33%), and light green for THF] at pH 7.

sharply as the salt concentration increased from 0.1 to 0.5 M and plateaued at higher concentrations (>0.5 M) (Table 2). Eventually, the enzyme showed maximal stability when the salt concentration reached 2 M, leading to an ∼8 °C increase in the melting temperature. Of the cosolvents investigated, methanol, ethanol, 2-propanol, and THF generally showed a destabilizing effect, with THF causing the greatest decrease in the melting temperature. While ethylene glycol has little influence on the thermostability of BsDHFR, the melting temperature increased slightly in the presence of glycerol and sucrose (Table 3). The protective and stabilizing effect of sugars and polyols against thermal denaturation and/or inactivation has also been observed in many other enzymes.[37−39] These compounds may partially internalize the surface hydrophobic residues and enhance hydrophobic interactions in the interior of the protein, allowing the protein to resist the thermal unfolding process.[40]

Table 2. Effect of Salts on the Melting Temperature of BsDHFR at pH 7

	T_m (°C)		
[salt] (M)	NaCl	KCl	KF
0.1	66.8 ± 0.2	66.9 ± 0.2	66.8 ± 0.2
0.2	67.2 ± 0.2	67.9 ± 0.2	67.5 ± 0.1
0.5	67.6 ± 0.2	68.3 ± 0.2	68.6 ± 0.2
1	69.5 ± 0.2	70.1 ± 0.2	71.0 ± 0.3
1.5	71.5 ± 0.4	71.7 ± 0.4	73.8 ± 0.8
2	73.4 ± 0.3	73.8 ± 0.3	74.6 ± 0.3

Table 3. Effects of Cosolvents on the Melting Temperature of BsDHFR at pH 7

	T_m (°C)		
	17% cosolvent	33% cosolvent	50% cosolvent
methanol	65.0 ± 0.3	48.7 ± 0.1	41.4 ± 0.2
ethanol	56.8 ± 0.1	45.1 ± 0.1	32.7 ± 0.2
2-propanol	55.2 ± 0.2	47.5 ± 0.6	43.4 ± 0.2
ethylene glycol	65.5 ± 0.2	67.5 ± 0.1	62.5 ± 0.2
glycerol	68.7 ± 0.2	72.5 ± 0.1	76.4 ± 0.1
sucrose	68.4 ± 0.2	71.8 ± 0.1	not determined
THF	44.8 ± 0.2	34.2 ± 0.8	not determined

Kinetics of BsDHFR and Variants. To understand how residues Leu20, Ala104, Pro122, and Pro129 affect BsDHFR catalysis, steady-state and hydride transfer rate constants were measured. The steady-state rate constants (k_{cat}) for the reduction of H_2F by NADPH were determined spectrophotometrically in the presence of excess substrate and cofactor. The k_{cat} for BsDHFR at pH 7 increased in an exponential fashion up to 65 °C but decreased at higher temperatures because of the thermal denaturation of the enzyme (Figure 4A). The k_{cat} for all variants increased exponentially up to only 55−60 °C. The k_{cat} values of BsDHFR-A104Q, BsDHFR-P122E, BsDHFR-P129D, and BsDHFR-P122E/P129D are similar to that of wild-type BsDHFR (Table 4). However, variants BsDHFR-L20M and BsDHFR-L20M/A104Q show an almost 2-fold decrease in the steady-state turnover numbers. In addition, all variants were further characterized by measuring the Michaelis constants for both NADPH and H_2F (Table 4). The K_M values of the variants are not markedly different from that of the wild type, except for those of BsDHFR-A104Q and BsDHFR-L20M/A104Q, which show K_M values for NADPH 5-fold lower than for the wild type. This is not unexpected, as Gln104 in MpDHFR and Gln102 in EcDHFR play a key role in NADPH binding by forming hydrogen bonds with its adenine moiety. Replacement of Gln104 with alanine in BsDHFR therefore compromises NADPH binding in favor of improved thermostability. These results suggest that the A104Q mutation affects binding but not turnover while the L20M mutation affects turnover but not binding. A likely explanation is that Leu20 is located in the center of the ligand binding sites and a slight change in residue size (e.g., replacement with the slightly longer

Table 1. Melting Temperatures of BsDHFR and Its Variants in 10 mM Potassium Phosphate Buffer at pH 7

enzyme	T_m (°C)	enzyme	T_m (°C)	enzyme	T_m (°C)
BsDHFR	66.2 ± 0.4	L20M	61.4 ± 0.1	P122E	65.3 ± 0.1
BsDHFR−NADPH	71.2 ± 0.4	A104Q	62.6 ± 0.1	P129D	64.6 ± 0.1
BsDHFR−H_2F	68.2 ± 0.4	L20M/A104Q	61.1 ± 0.1	P122E/P129D	65.0 ± 0.1

dx.doi.org/10.1021/bi500238q | *Biochemistry* 2014, 53, 2855−2863

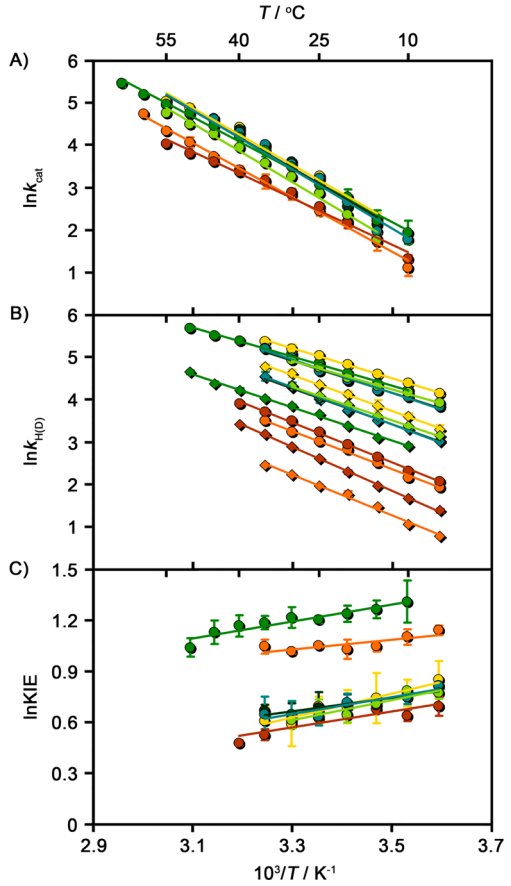

Figure 4. Arrhenius plots of (A) the steady-state rate constants, (B) the hydride (circles) and deuteride (diamonds) transfer rate constants, and (C) the corresponding KIEs on a logarithmic scale against the inverse temperature for BsDHFR and its variants for the catalyzed reaction at pH 7: green for wild-type BsDHFR, orange for BsDHFR-L20M, gold for BsDHFR-A104Q, brown for BsDHFR-L20M/A104Q, dark green for BsDHFR-P122E, teal for BsDHFR-P129D, and yellow-green for BsDHFR-P122E/P129D.

residue Met) might lead to a subtle distortion in the active site, which is sufficient to decrease the rate of steady-state turnover but because of its position does not affect substrate binding. The presence of Leu20 is therefore beneficial to both thermostability and catalysis. All the mutations change the activation energy of the BsDHFR-catalyzed turnover only moderately (Table 4), suggesting that the catalytic cycle is not significantly affected.

The chemical step in BsDHFR and each variant was interrogated using a stopped-flow experimental setup to measure the rate constant for hydride transfer (k_H). In general, k_H in the BsDHFR variants increased exponentially to approximately 35−40 °C (Figure 4B). The k_H of the wild-type enzyme, in contrast, increased exponentially to 50 °C. Similar to k_{cat}, the k_H values are much lower in BsDHFR-L20M and BsDHFR-L20M/A104Q, likely because of the subtle distortion of the active site as discussed above. The measured hydride transfer rate constants in BsDHFR-A104Q, BsDHFR-P122E, BsDHFR-P129D, and BsDHFR-P122E/P129D are at least 1 order of magnitude greater than the steady-state turnover rates at low temperatures (<25 °C), implying that the actual reduction of the substrate is not the rate-limiting step. As the temperature increases, the chemical step becomes partially rate-limiting, providing hydride transfer rates that are only 3−4 times higher than the turnover rates. In contrast, the chemical step in BsDHFR-L20M and BsDHFR-L20M/A104Q is partially rate-limiting across the whole temperature range; the hydride transfer rate constants are only 2−3 times higher than the steady-state turnover rate. Additionally, the mutation of Leu20 to methionine leads to an increase in the activation energy (Table 5). The kinetic isotope effects (KIEs) on k_H were also measured for all the BsDHFR variants. While the observed KIEs for all the BsDHFR variants decreased slightly, these mutations did not affect the temperature dependence of the KIE (Figure 4C).

Effect of Salt on BsDHFR Catalysis. NaCl, KCl, and KF all gave a maximal specific activity of BsDHFR at 0.1 M but showed inhibitory effects above this concentration (Figure 5A). The inhibitory effect of KF was strongest. At 1 M NaCl, the activity of BsDHFR was nearly 80% lower than in buffer without salt, while the enzyme lost >90% of its initial activity in the presence of 2 M NaCl. This effect was also observed for NaCl by Kim et al.[19] In contrast, the hydride transfer rate constant of BsDHFR was increased significantly by NaCl and KCl across the concentration range studied at both room temperature and elevated temperature (Figure 5B), so hydride transfer remained a fast, non-rate-limiting step in the reaction. The addition of 2 M NaCl increases k_H by 267 and 99% at 20 and 40 °C, respectively, while the effect of KCl is less pronounced; KF causes a slight increase in k_H to ∼1.0 M but a subsequent decrease in k_H above 1.5 M. The three salts all had little effect on the KIE, which remained constant for salt concentrations up to 1 M but decreased slightly at concentrations above 1.5 M. It is not certain whether high-ionic strength buffers represent the naturally functioning environment of BsDHFR. The optimal growth NaCl concentration of *G. stearothermophilus* is relatively low (∼85 mM),[41] but the effect of molecular crowding within the cell may lead to a relatively high ionic strength.

Effect of Cosolvent on BsDHFR Catalysis. The k_{cat} at 20 °C and the k_H at 20 and 40 °C for the BsDHFR-catalyzed reaction were measured in the presence of organic cosolvents (Figure 6). Generally, increasing concentrations of cosolvents

Table 4. k_{cat} Values and Activation Parameters of BsDHFR and Its Variants and Their K_M Values at 20 °C and pH 7

enzyme	k_{cat} (20 °C) (s^{-1})	E_a^H (kJ mol^{-1})	A_H ($\times 10^{10}$ s^{-1})	K_M (NADPH) (μM)	K_M (H_2F) (μM)
BsDHFR	16.2 ± 2.8	51.6 ± 1.6	2.51 ± 0.06	108 ± 28	2.4 ± 0.4
BsDHFR-L20M	9.03 ± 1.31	52.9 ± 1.3	2.70 ± 0.06	114 ± 29	2.6 ± 0.5
BsDHFR-A104Q	15.2 ± 1.5	55.1 ± 2.5	14.4 ± 0.5	21.6 ± 2.4	2.1 ± 0.3
BsDHFR-L20M/A104Q	8.69 ± 0.74	45.2 ± 1.7	0.12 ± 0.01	15.3 ± 1.6	3.2 ± 0.7
BsDHFR-P122E	13.0 ± 0.2	56.0 ± 3.5	18.7 ± 0.10	105 ± 20	1.6 ± 0.4
BsDHFR-P129D	14.5 ± 1.2	57.5 ± 3.0	33.3 ± 1.5	107 ± 22	2.5 ± 0.3
BsDHFR-P122E/P129D	10.6 ± 0.4	57.1 ± 2.4	20.8 ± 0.8	126 ± 21	3.1 ± 0.9

dx.doi.org/10.1021/bi500238q | *Biochemistry* 2014, 53, 2855−2863

Table 5. k_H and KIE Values at 20 °C and Activation Parameters for Hydride Transfer Catalyzed by BsDHFR and Its Variants at pH 7

enzyme	k_H (20 °C) (s^{-1})	KIE (20 °C)	E_a^H (kJ mol^{-1})	ΔE_a (kJ mol^{-1})	A_H ($\times 10^7$ s^{-1})	A_H/A_D
BsDHFR	102 ± 5	3.44 ± 0.17	28.1 ± 0.8	3.3 ± 1.0	1.02 ± 0.02	0.87 ± 0.02
BsDHFR-L20M	16.7 ± 0.1	2.80 ± 0.16	37.5 ± 1.0	2.3 ± 1.8	7.80 ± 0.18	1.10 ± 0.05
BsDHFR-A104Q	125 ± 8	2.00 ± 0.19	29.3 ± 0.5	5.8 ± 1.0	2.05 ± 0.03	0.18 ± 0.01
BsDHFR-L20M/A104Q	19.0 ± 0.1	1.90 ± 0.08	39.1 ± 0.9	3.9 ± 1.0	17.2 ± 0.3	0.38 ± 0.01
BsDHFR-P122E	84.8 ± 3.7	2.02 ± 0.12	31.7 ± 1.6	3.3 ± 1.9	4.01 ± 0.15	0.52 ± 0.02
BsDHFR-P129D	86.4 ± 3.8	2.05 ± 0.10	32.4 ± 1.5	4.1 ± 2.0	5.48 ± 0.19	0.38 ± 0.02
BsDHFR-P122E/P129D	92.2 ± 3.3	1.89 ± 0.08	27.9 ± 0.9	4.9 ± 1.0	0.90 ± 0.02	0.26 ± 0.01

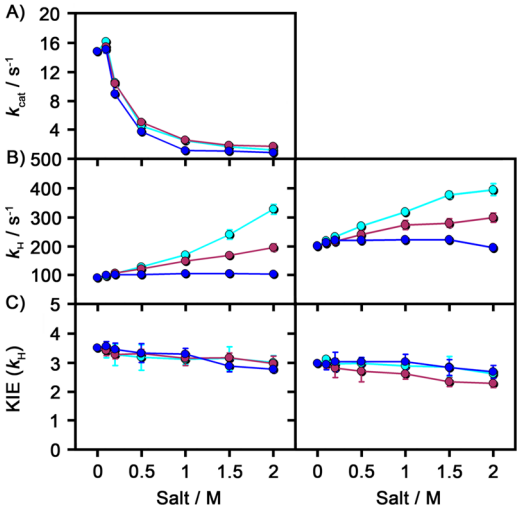

Figure 5. Effect of ionic strength on (A) the steady-state rate constant of BsDHFR at 20 °C, (B) the pre-steady-state rate constant at 20 °C (left) and 40 °C (right), and (C) the corresponding KIEs. The buffer was 100 mM K_iPO_4 (pH 7) in the presence of NaCl (cyan), KCl (purple), and KF (blue).

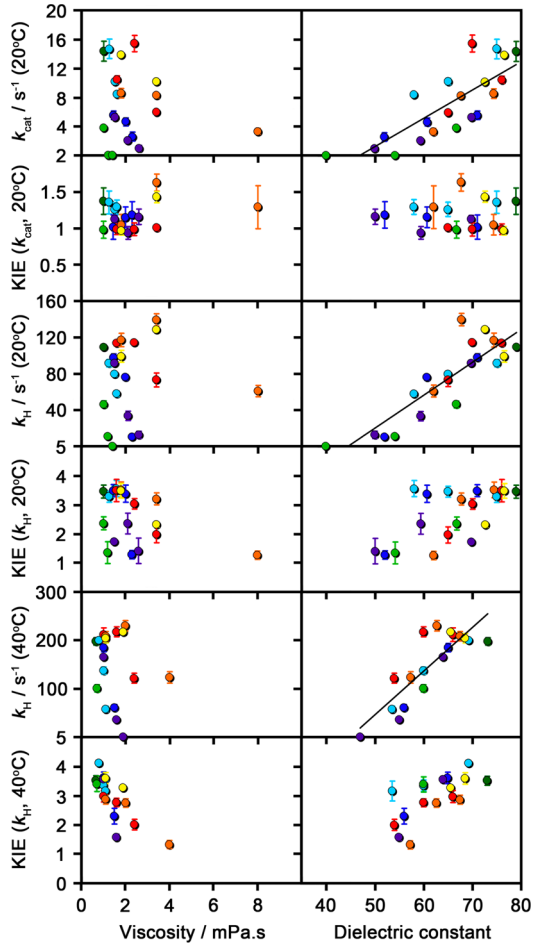

Figure 6. Plots of k_{cat}, k_H, and their KIEs against solution viscosity (left) and dielectric constant (right). Symbols represent the different cosolvents, where green denotes no cosolvent, light blue methanol, dark blue ethanol, purple 2-propanol, red ethylene glycol, orange glycerol, yellow sucrose, and light green THF. In the case of dielectric constant data, lines of best fit are shown.

led to decreases in both rate constants, but CD spectroscopy showed that the secondary structure of BsDHFR is maintained (*vide supra*). It is therefore likely that the reduction of the rate constants is not related to solvent-induced structural changes. Similar to the effect previously observed for MpDHFR,[34] EcDHFR,[36] and DHFR from the hyperthermophile *Thermotoga maritima* (TmDHFR),[32] the values of k_H and k_{cat} were not reduced in a manner directly proportional to the medium viscosity but were decreased in a manner proportional to the dielectric constant. The k_H and k_{cat} values decreased to zero when the dielectric constant of the solvent was less than ~50. The decrease in k_{cat} and k_H with a decreasing dielectric constant can be interpreted as an indication that the dielectric constant affects catalysis by influencing the shielding of stabilizing electrostatic effects within the active site.[32,36] As has also been observed for other DHFRs,[32,34,36] the KIE on both k_H and k_{cat} did not change proportionally with the solvent properties. Although DHFRs with different thermal stabilities show different flexibility and structural stability in cosolvents, their kinetic behavior in organic cosolvents is essentially the same. Therefore, as seen for MpDHFR[34] and EcDHFR,[36] it appears that large-scale, nonlocal motions are not directly coupled to hydride transfer in BsDHFR.

CONCLUSIONS

BsDHFR is a moderately thermophilic enzyme. Its melting temperature was determined to be 66.2 ± 0.4 °C, and its steady-state and pre-steady-state rate constants reach maxima around this temperature. Additional thermostability of BsDHFR can be obtained by the addition of ligands, salts, or cosolvents such as glycerol and sucrose. It has been suggested that the thermostability of BsDHFR might be enhanced by extra proline residues located in loop regions.[19] However, replacing Pro122 and Pro129 in the FG loop with acidic residues did not significantly affect the melting temperature. Moreover, there are fewer thermolabile residues, such as methionine, asparagine, and glutamine, in BsDHFR. Incorporation of thermolabile methionine or glutamine residues had a stronger effect on the thermostability of BsDHFR than removal

dx.doi.org/10.1021/bi500238q | *Biochemistry* 2014, 53, 2855−2863

of proline residues. Replacing Leu20 with methionine caused a 5 °C decrease in the melting temperature of BsDHFR, while replacing Ala104 with glutamine caused a 3 °C decrease in the melting temperature but strengthened NADPH binding considerably.

In contrast, the K_M for NADPH of TmDHFR is much lower than those of other DHFRs, indicating very strong NADPH binding.[42] Because NADPH is quite unstable at the optimal working temperature of TmDHFR (80 °C),[43] the tight binding of NADPH in the active site can stabilize both the enzyme and the cofactor. Tight ligand binding has been observed in various hyperthermophilic enzymes, whose optimal working temperature is >80 °C.[44−46] As NADPH is considerably more stable at the optimal working temperature of BsDHFR (60 °C), BsDHFR can compromise its affinity for NADPH in favor of improved thermostability.

The strategy for thermal adaptation of moderately thermophilic BsDHFR is considerably different from that of hyperthermophilic TmDHFR. The lower limit of the working temperature of BsDHFR *in vivo* (30 °C)[26] is close to the optimal working temperature of mesophilic EcDHFR (37 °C), and the catalytic activity of BsDHFR is comparable to that of EcDHFR, likely because both enzymes can adopt the closed conformation.[19] In EcDHFR, the ability to adopt the closed conformation is crucial for catalysis, as it forms an ideal electrostatic and geometric environment for hydride transfer.[23] On the other hand, crystallographic studies revealed that TmDHFR can adopt only an open conformation,[47] because it forms a highly stable homodimer and the loops corresponding to those involved in conformational changes in EcDHFR are buried in the dimer interface instead. This likely prevents an ideal electrostatic preorganization, as it exposes the active site to solvent molecules, and makes TmDHFR almost inactive at low temperatures.[48] However, dimerization is the main mechanism by which TmDHFR achieves its extreme thermostability.[49] In contrast, thermal adaptation of BsDHFR is attained by the removal of thermolabile residues as well as rigidification of certain parts of the enzyme (the M20, FG, and GH loops as well as the protein core).[21] We have shown previously that monomerization of TmDHFR and dimerization of EcDHFR do not give opposite effects and, therefore, that TmDHFR cannot be considered simply as a dimer of a monomeric DHFR.[50]

In conclusion, elongation of secondary structure elements observed previously[19] and the replacement of water-accessible thermolabile residues with simple hydrophobic amino acids appear to be the key contributors to the thermostability of BsDHFR, whereas the addition of proline residues to loop regions plays only a more minor role. However, in addition to the intrinsic thermostability conferred by its amino acid sequence, additional stabilizing factors such as ligand binding and interactions with salts and/or organic compounds such as glycerol and sucrose must help BsDHFR achieve the necessary stability *in vivo* to function at temperatures above 70 °C. In general, catalysis by BsDHFR is very similar to that of other monomeric DHFRs, despite having a melting temperature more similar to that of TmDHFR than that of MpDHFR, reinforcing TmDHFR's position as a special case. It would be interesting to discover at what temperature dimerization becomes a necessary mechanism for ensuring stability in hyperthermophilic DHFRs.

■ ASSOCIATED CONTENT

Supporting Information

Temperature dependence of k_{cat}, k_H, k_D, and KIE(k_H) of BsDHFR and its variants; effect of salt on the k_{cat} of BsDHFR at 20 °C; effect of salt on the k_H and KIE(k_H) of BsDHFR at 20 and 40 °C; effect of solvent on the k_{cat} and KIE(k_{cat}) of BsDHFR at 20 °C; and effect of solvent on the k_H and KIE(k_H) of BsDHFR at 20 and 40 °C. This material is available free of charge via the Internet at http://pubs.acs.org.

■ AUTHOR INFORMATION

Corresponding Author

*School of Chemistry, Cardiff University, Main Building, Park Place, Cardiff CF10 3AT, United Kingdom. E-mail: allemannrk@cf.ac.uk. Phone: (44) 29 2087 4805. Fax: (44) 29 2087 4030.

Author Contributions

J.G. performed all the experimental work and wrote the manuscript. L.Y.P.L., E.J.L. and R.K.A. designed the experiments. All authors contributed to the final manuscript.

Funding

This work was supported by Grant BB/J005266/1 (R.K.A.) from the UK Biotechnology and Biological Sciences Research Council and the Vice Chancellor Fund of Cardiff University.

Notes

The authors declare no competing financial interest.

■ ABBREVIATIONS

DHFR, dihydrofolate reductase; BsDHFR, DHFR from *G. stearothermophilus*; EcDHFR, DHFR from *E. coli*; MpDHFR, DHFR from *M. profunda*; TmDHFR, DHFR from *T. maritima*; NADPH, nicotinamide adenine dinucleotide phosphate; H_2F, 7,8-dihydrofolate; H_4F, 5,6,7,8-tetrahydrofolate; KIE, kinetic isotope effect; OD, optical density; IPTG, isopropyl β-D-thiogalactopyranoside; CD, circular dichroism; MRE, mean residue ellipticity; FRET, fluorescence resonance energy transfer; THF, tetrahydrofuran; PDB, Protein Data Bank.

■ REFERENCES

(1) Russell, R. J. M., Ferguson, J. M. C., Hough, D. W., Danson, M. J., and Taylor, G. L. (1997) The crystal structure of citrate synthase from the hyperthermophilic archaeon *Pyrococcus* furiosus at 1.9 Å resolution. *Biochemistry 36*, 9983−9994.

(2) Haney, P., Konisky, J., Koretke, K. K., Luthey-Schulten, Z., and Wolynes, P. G. (1997) Structural basis for thermostability and identification of potential active site residues for adenylate kinases from the archaeal genus *Methanococcus*. *Proteins 28*, 117−130.

(3) Zuber, H. (1988) Temperature adaptation of lactate dehydrogenase structure, functional and genetic aspects. *Biophys. Chem. 29*, 171−179.

(4) Russell, R. J. M., Gerike, U., Danson, M. J., Hough, D. W., and Taylor, G. L. (1998) Structural adaptations of the cold-active citrate synthase from an antarctic bacterium. *Structure 6*, 351−361.

(5) Vogt, G., and Argos, P. (1997) Protein thermal stability: Hydrogen bonds or internal packing? *Folding Des. 2*, S40−S46.

(6) Vogt, G., Woell, S., and Argos, P. (1997) Protein thermal stability, hydrogen bonds, and ion pairs. *J. Mol. Biol. 269*, 631−643.

(7) Salminen, T., Teplyakov, A., Kankare, J., Cooperman, B. S., Lahti, R., and Goldman, A. (1996) An unusual route to thermostability disclosed by the comparison of *Thermus thermophilus* and *Escherichia coli* inorganic pyrophosphatases. *Protein Sci. 5*, 1014−1025.

(8) Yip, K. S. P., Stillman, T. J., Britton, K. L., Artymiuk, P. J., Baker, P. J., Sedelnikova, S. E., Engel, P. C., Pasquo, A., Chiaraluce, R., Consalvi, V., Scandurra, R., and Rice, D. W. (1995) The structure of

Pyrococcus furiosus glutamate-dehydrogenase reveals a key role for ion-pair networks in maintaining enzyme stability at extreme temperatures. *Structure 3*, 1147−1158.
(9) Yip, K. S. P., Britton, K. L., Stillman, T. J., Lebbink, J., De Vos, W. M., Robb, F. T., Vetriani, C., Maeder, D., and Rice, D. W. (1998) Insights into the molecular basis of thermal stability from the analysis of ion-pair networks in the glutamate dehydrogenase family. *Eur. J. Biochem. 255*, 336−346.
(10) Elcock, A. H. (1998) The stability of salt bridges at high temperatures: Implications for hyperthermophilic proteins. *J. Mol. Biol. 284*, 489−502.
(11) Xiao, L., and Honig, B. (1999) Electrostatic contributions to the stability of hyperthermophilic proteins. *J. Mol. Biol. 289*, 1435−1444.
(12) Kumar, S., Ma, B. Y., Tsai, C. J., and Nussinov, R. (2000) Electrostatic strengths of salt bridges in thermophilic and mesophilic glutamate dehydrogenase monomers. *Proteins 38*, 368−383.
(13) Watanabe, K., Hata, Y., Kizaki, H., Katsube, Y., and Suzuki, Y. (1997) The refined crystal structure of *Bacillus cereus* oligo-1,6-glucosidase at 2.0 Å resolution: Structural characterization of proline-substitution sites for protein thermostabilization. *J. Mol. Biol. 269*, 142−153.
(14) Bogin, O., Peretz, M., Hacham, Y., Korkhin, Y., Frolow, F., Kalb, A. J., and Burstein, Y. (1998) Enhanced thermal stability of *Clostridium beijerinckii* alcohol dehydrogenase after strategic substitution of amino acid residues with prolines from the homologous thermophilic *Thermoanaerobacter brockii* alcohol dehydrogenase. *Protein Sci. 7*, 1156−1163.
(15) Charlton, P. A., Young, D. W., Birdsall, B., Feeney, J., and Roberts, G. C. K. (1979) Stereochemistry of reduction of folic-acid using dihydrofolate-reductase. *J. Chem. Soc., Chem. Commun.*, 922−924.
(16) Charlton, P. A., Young, D. W., Birdsall, B., Feeney, J., and Roberts, G. C. K. (1985) Stereochemistry of reduction of the vitamin folic-acid by dihydrofolate-reductase. *J. Chem. Soc., Perkin Trans. 1*, 1349−1353.
(17) Donk, P. J. (1920) A highly resistant thermophilic organism. *J. Bacteriol. 5*, 373−374.
(18) Nazina, T. N., Tourova, T. P., Poltaraus, A. B., Novikova, E. V., Grigoryan, A. A., Ivanova, A. E., Lysenko, A. M., Petrunyaka, V. V., Osipov, G. A., Belyaev, S. S., and Ivanov, M. V. (2001) Taxonomic study of aerobic thermophilic Bacilli: Descriptions of *Geobacillus subterraneus* gen. nov., sp. nov and *Geobacillus uzenensis* sp. nov from petroleum reservoirs and transfer of *Bacillus stearothermophilus*, *Bacillus thermocatenulatus*, *Bacillus thermoleovorans*, *Bacillus kaustophilus*, *Bacillus thermoglucosidasius* and *Bacillus thermodenitrificans* to *Geobacillus* as the new combinations *G. stearothermophilus*, *G. thermocatenulatus*, *G. thermoleovorans*, *G. kaustophilus*, *G. thermoglucosidasius* and *G. thermodenitrificans*. *Int. J. Syst. Evol. Microbiol. 51*, 433−446.
(19) Kim, H. S., Damo, S. M., Lee, S. Y., Wemmer, D., and Klinman, J. P. (2005) Structure and hydride transfer mechanism of a moderate thermophilic dihydrofolate reductase from *Bacillus stearothermophilus* and comparison to its mesophilic and hyperthermophilic homologues. *Biochemistry 44*, 11428−11439.
(20) Meinhold, L., Clement, D., Tehei, M., Daniel, R., Finney, J. L., and Smith, J. C. (2008) Protein dynamics and stability: The distribution of atomic fluctuations in thermophilic and mesophilic dihydrofolate reductase derived using elastic incoherent neutron scattering. *Biochem. J. 94*, 4812−4818.
(21) Oyeyemi, O. A., Sours, K. M., Lee, T., Resing, K. A., Ahn, N. G., and Klinman, J. P. (2010) Temperature dependence of protein motions in a thermophilic dihydrofolate reductase and its relationship to catalytic efficiency. *Proc. Natl. Acad. Sci. U.S.A. 107*, 10074−10079.
(22) Oyeyemi, O. A., Sours, K. M., Lee, T., Kohen, A., Resing, K. A., Ahn, N. G., and Klinman, J. P. (2011) Comparative hydrogen-deuterium exchange for a mesophilic vs thermophilic dihydrofolate reductase at 25 °C: Identification of a single active site region with enhanced flexibility in the mesophilic protein. *Biochemistry 50*, 8251−8260.
(23) Sawaya, M. R., and Kraut, J. (1997) Loop and subdomain movements in the mechanism of *Escherichia coli* dihydrofolate reductase: Crystallographic evidence. *Biochemistry 36*, 586−603.
(24) Bystroff, C., and Kraut, J. (1991) Crystal structure of unliganded *Escherichia coli* dihydrofolate reductase. Ligand induced conformational changes and cooperativity in binding. *Biochemistry 30*, 2227−2239.
(25) Evans, R. M., Behiry, E. M., Tey, L.-H., Guo, J., Loveridge, E. J., and Allemann, R. K. (2010) Catalysis by dihydrofolate reductase from the psychropiezophile *Moritella profunda*. *ChemBioChem 11*, 2010−2017.
(26) Hashizume, S., Sekiguchi, T., and Nosoh, Y. (1976) Effect of temperature on viability of *Bacillus stearothermophilus*. *Arch. Microbiol. 107*, 75−80.
(27) Loveridge, E. J., and Allemann, R. K. (2011) Effect of pH on hydride transfer by *Escherichia coli* dihydrofolate reductase. *ChemBioChem 12*, 1258−1262.
(28) Zakrzewski, S. F. (1966) On mechanism of chemical and enzymatic reduction of folate and dihydrofolate. *J. Biol. Chem. 241*, 2962−2967.
(29) Fierke, C. A., Johnson, K. A., and Benkovic, S. J. (1987) Construction and evaluation of the kinetic scheme associated with dihydrofolate reductase from *Escherichia coli*. *Biochemistry 26*, 4085−4092.
(30) Swanwick, R. S., Maglia, G., Tey, L.-H., and Allemann, R. K. (2006) Coupling of protein motions and hydrogen transfer during catalysis by *Escherichia coli* dihydrofolate reductase. *Biochem. J. 394*, 259−265.
(31) Pace, C. N., Vajdos, F., Fee, L., Grimsley, G., and Gray, T. (1995) How to measure and predict the molar absorption coefficient of a protein. *Protein Sci. 4*, 2411−2423.
(32) Loveridge, E. J., Evans, R. M., and Allemann, R. K. (2008) Solvent effects on environmentally coupled hydrogen tunnelling during catalysis by dihydrofolate reductase from *Thermotoga maritima*. *Chem.—Eur. J. 14*, 10782−10788.
(33) Stone, S. R., and Morrison, J. F. (1982) Kinetic mechanism of the reaction catalyzed by dihydrofolate reductase from *Escherichia coli*. *Biochemistry 21*, 3757−3765.
(34) Loveridge, E. J., Tey, L.-H., Behiry, E. M., Dawson, W. M., Evans, R. M., Whittaker, S. B.-M., Gunther, U. L., Williams, C., Crump, M. P., and Allemann, R. K. (2011) The role of large-scale motion in catalysis by dihydrofolate reductase. *J. Am. Chem. Soc. 133*, 20561−20570.
(35) Kumar, S., Tsai, C. J., and Nussinov, R. (2000) Factors enhancing protein thermostability. *Protein Eng. 13*, 179−191.
(36) Loveridge, E. J., Tey, L.-H., and Allemann, R. K. (2010) Solvent effects on catalysis by *Escherichia coli* dihydrofolate reductase. *J. Am. Chem. Soc. 132*, 1137−1143.
(37) Back, J. F., Oakenfull, D., and Smith, M. B. (1979) Increased thermal stability of proteins in the presence of sugars and polyols. *Biochemistry 18*, 5191−5196.
(38) Hédoux, A., Willart, J. F., Ionov, R., Affouard, F., Guinet, Y., Paccou, L., Lerbret, A., and Descamps, M. (2006) Analysis of sugar biopretective mechanisms on the thermal denaturation of lysozyme from Raman scattering and differential scanning calorimetry investigations. *J. Phys. Chem. B 110*, 22886−22893.
(39) Yadav, J. K., and Prakash, V. (2009) Thermal stability of α-amylase in aqueous cosolvent systems. *J. Biosci. 34*, 377−387.
(40) Sola-Penna, M., and Meyer-Fernandes, J. R. (1998) Stabilization against thermal inactivation pronoted by sugars on enzyme structure and function: Why is the trehalose more effective than other sugars? *Arch. Biochem. Biophys. 360*, 10−14.
(41) Ng, T. M., and Schaffner, D. W. (1997) Mathematical models for the effects of pH, temperature, and sodium chloride on the growth of *Bacillus stearothermophilus* in salty carrots. *Appl. Environ. Microbiol. 63*, 1237−1243.
(42) Maglia, G., Javed, M. H., and Allemann, R. K. (2003) Hydride transfer during catalysis by dihydrofolate reductase from *Thermotoga maritima*. *Biochem. J. 374*, 529−535.

(43) Walsh, K. A. J., Daniel, R. M., and Morgan, H. W. (1983) A soluble NADH dehydrogenase (NADH:ferricyanide oxidoreductase) from *Thermus aquaticus* strain T351. *Biochem. J. 209*, 427−433.
(44) Koch, R., Canganella, F., Hippe, H., Jahnke, K. D., and Antranikian, G. (1997) Purification and properties of a thermostable pullulanase from a newly isolated thermophilic anaerobic bacterium, *Fervidobacterium pennavorans* Ven5. *Appl. Environ. Microbiol. 63*, 1088−1094.
(45) Klingeberg, M., Galunsky, B., Sjoholm, C., Kasche, V., and Antranikian, G. (1995) Purification and properties of a highly thermostable, sodium dodecyl sulfate-resistant and stereospecific proteinase from the extremely thermophilic archaeon *Thermococcus stetteri*. *Appl. Environ. Microbiol. 61*, 3098−3104.
(46) Andreotti, G., Cubellis, M. V., Nitti, G., Sannia, G., Mai, X. H., Adams, M. W. W., and Marino, G. (1995) An extremly thermostable aromatic aminotransferase from the hyperthermophilic archaeon *Pyrococcus furiosus*. *Biochim. Biophys. Acta 1247*, 90−96.
(47) Dams, T., Auerbach, G., Bader, G., Jacob, U., Ploom, T., Huber, R., and Jaenicke, R. (2000) The crystal structure of dihydrofolate reductase from *Thermotoga maritima*: Molecular features of thermostability. *J. Mol. Biol. 297*, 659−672.
(48) Loveridge, E. J., Maglia, G., and Allemann, R. K. (2009) The role of arginine 28 in catalysis by dihydrofolate reductase from the hyperthermophile *Thermotoga maritima*. *ChemBioChem 10*, 2624−2627.
(49) Loveridge, E. J., Rodriguez, R. J., Swanwick, R. S., and Allemann, R. K. (2009) Effect of dimerization on the stability and catalytic activity of dihydrofolate reductase from the hyperthermophile *Thermotoga maritima*. *Biochemistry 48*, 5922−5933.
(50) Guo, J., Loveridge, E. J., Luk, L. Y. P., and Allemann, R. K. (2013) Effect of Dimerization on Dihydrofolate Reductase Catalysis. *Biochemistry 52*, 3881−3887.
(51) Thompson, J. D., Higgins, D. G., and Gibson, T. J. (1994) CLUSTAL W: Improving the sensitivity of progressive multiple sequence alignment through sequence weighting, position-specific gap penalties and weight matrix choice. *Nucleic Acids Res. 22*, 4673−4680.